Synthesis and Characterization of Au:CuO Nanocomposite by Laser Soldering on Porous Silicon for Photodetector

Halah H. Rashed* and Juhaina Moatasemballah
Department of Applied Science, University of Technology, Baghdad-Iraq.
*Corresponding Author: hala_hassan8140@yahoo.com.

Abstract

This work aimed to the synthesize of composite Au:CuO (NPs) by pulsed laser soldering process. The optical properties, stability, structural properties and surface morphology of Au:CuO nanocomposite were characterized by UV–VIS spectrophotometer, Zeta potential measurement, X-Ray Diffraction pattern and Atomic Force Microscope respectively. The band gap of Au doped CuO is about 1.95 eV. The amount of zeta potential is -54 mV, its indicating that the negatively charged of Au: CuO nanocomposite in deionized water and the colloid is good stability against aggregation. Surface morphology of Au:CuO nanocomposite show a large number of particles have diameter about 55nm.

Au: CuO nanocomposite deposited on porous silicon by drop casting technique for preparation of silicon photodetector, the electrical properties prove that band gap alignment between Au: CuO nanocomposite and PS facilitates the electron transfer and further increases the photoresponsitivity and Quantum efficiency. [DOI: 10.22401/JUNS.20.2.07]

Keywords: Au:CuO nanocomposite, Zetapotential, Au:CuO/porous silicon hetrojunction.

Introduction

Nanocomposites (NC) are dispersed phase formed by metallic or metallic oxides nanoparticles in a matrix which can be amorphous or crystalline, it have gained increasing attention because of the new physics of the two phases heterojunctions which can lead to improved physical and mechanical properties [1]. The nanocomposite formed from the metal oxide and nobel metal such as (Au, Ag) is the perfect choice to change the electrical, mechanical and optical properties of these material [2]. Different technique used in fabrication of nanocomposite deposition-precipitation method [3], combining hydrothermal and electric beam evaporation deposition method [4], novel chemical vapor deposition (CVD) route [5], pulse laser deposition [6], Among these methods; pulsed laser ablation in liquid technique (PLAL) used to synthesis of nanocomposite. This method is simple, cheap, clean, one step procedure and can controble technique for prepration of nanoparticles with specific properties depend on the preparation conditions and laser parameters [7]. Several nanocomposite such as Au/SnO_2 [7], Au /Ag [8], Fe/Au [9], Fe/Pt [10], and Au/ZnO, Au/CuO [1] have been successively synthesized by laser ablation in liquid. Composite gold and copper oxide (Au/CuO) is very important because it has many advantages, Au favored very stable, catalytic effectiveness and relatively good conductive [11], copper oxide as a transition metal oxide, It is a p-type semiconductor with a narrow direct band gap of 1.2 eV, not poisonous material and relatively good electrical and optical properties [12], Au/CuO has many application such as glucose sensor because it's exhibited good catalytic activity for CO oxidation, good non-enzymatic sensitivity for glucose [13] and surface enhanced Raman scattering and clock reaction [14]. Porous silicon (PS) can be enhance the conversion efficiency of solar cell, PS is a promising one as it has the capability of a wide absorption bands and high transmission from 700 to 1000nm. The most important advantages of using porous silicon in solar cells are its textured nature surface which traps light and reduces the reflectance losses, tuning of band gap for optimum sunlight absorption, conversion into direct band gap semiconductor with large quantum efficiency [15].

Experimental work

A) Material preparation

I) Synthesis of Au : CuO nanocomposite

Composite Au:CuO synthesized by multi step process. First step: Au and CuO nanoparticle prepared by pulsed laser ablation of Au and Cu foils in deionized water (DIW). This method is prepared by immersed the Au and Cu plates (purity of 99.99%) in 3 ml of DIW in separate plastic container. A Q-switching Nd: YAG laser at 1064 nm wavelength with 350 mJ laser energy, 500 laser pulses and 7 nsec pulse duration is focused vertically aligned on the target with lens have 10 cm focal length. Fig.(1(a)) show the schematic diagram of laser ablation in DIW. During laser ablation, the color of Au colloid is slowly converted to pink after 250 laser pulses, While CuO colloid is transparent but progressively converts to light green color after 500 pulses, these phenomena matched the cases of the formation of nanoparticles by laser ablation, The optical images of gold and copper oxide colloids are shown in the Fig.(1(b)).

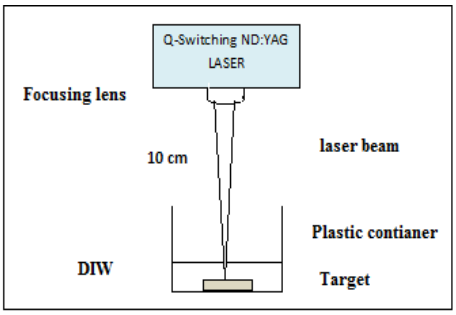

(a)

Gold nanoparticle Copper oxide nanoparticle

(b)

Fig.(1): (a) Schematic diagram of laser ablation in DIW. (b) The optical images of gold and copper oxide nanoparticle respectively.

Second step: post-ablation laser heating of mixed solution of Au colloidal and CuO colloidal to form nanocomposite at 350 mJ laser eergy,1.06 μm laser wavelength and 250 laser pulses. The optical properties of Au, CuO and Au: CuO nanocomposite characterized by double beam UV-Visible spectrophotometer (Shimadzu) with 1 cm optical length of the cell; The stability of Au: CuO nanocomposite measured using by Zeta Plus Signal Processing analyzer, its work by Electrophoretic Light Scattering (ELS) by red diode laser with 35 mW power and 640 nm wavelength, the potential was determined based on the velocity of the particles in a unit electric field, Then the structural properties and surface morphology characterized by X-Ray diffraction and Atomic Force Microscope (AFM) respectively.

II) Synthesis porous silicon by photo electrochemical etching

Porous silicon prepared by photo electrochemical etching by using green laser at 532 nm wavelength and power 30 mW. N-type Silicon with resistivity of 4-10cm and (100) orientation were used as starting substrate. Its rectangle shape with areas 1 cm^2, the unwanted oxide layer is removed through submerged with a solution resulting from the mixing of hedrofloriek and DIW with ratio of (1: 2). After chemical treatment, Green laser of Si wafer is used: HF-ethanol (measured by volume) aqua's with 25% concentration at room temperature by using a Pt electrode in a normal etching Teflon cell. The applying current during etching was 10 mA for 3 min etching time. Fig.(2) demonstrate the schematic diagram of photo chemical method.

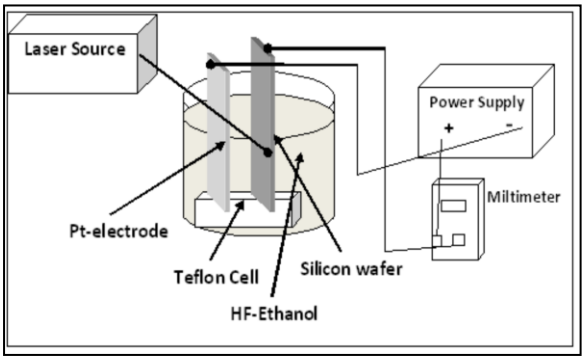

Fig.(2): Schematic diagram of photo chemical method.

After iodization, PS sample is carefully removed from the bath and cleaned in deionized water and acetone to remove the black wax mask. Then the sample imaged by Atomic Force Microscope (AFM).

B) Characterization of Au:CuO nanocomposite/porous silicon hetrojunction

Photo detector was prepared by deposition Au: CuO nanocomposite on the porous silicon by drop casting technique. These particles covered the pore walls of porous silicon matrix. After deposition, Aluminum with purity (99.99%) thin film was deposited as back and silver paste on the forth surface for the fabricated sample for ohmic contact.

Results and Discussions

I- Characterization of Au: CuO nanocomposite

1- Optical properties

UV-Visible-NIR absorption spectrophoto-meter was used to characterize the optical properties of nanoparticle, since the absorption band is related to the diameter and aspect ratio of the nanoparticle [1]. The optical absorption spectra of Au and CuO colloids are illustrative in Fig.(3) and Fig.(4) respectively. Fig.(3) indicates the absorption spectrum of gold colloidal prepared by laser ablation in DIW. This spectrum shows a maximum peak at 526 nm, which corresponds to the surface Plasmon resonance and its originating from the interband transitions of gold nanoparticles [16], this phenomena appears on the surface of some of the minerals, a result of collective motion of free electrons at the nanoscale particle of incident light upon it, a movement periodical where the direction of the electron with the times is changing with the same frequency of the incident electromagnetic wave [17].

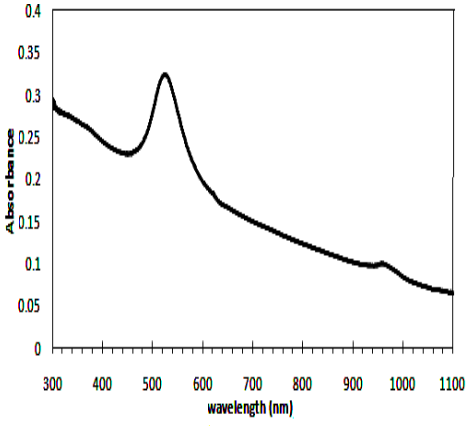

Fig.(3): Absorption spectrum as a function of wavelength of Au nanoparticles synthesis by laser ablation in DIW.

Fig.(4(a)) illustrates the absorption spectrum of CuO nanoparticles prepared by laser ablation in DIW, a series of peaks could be recognize, the absorption peak from (260 to 340 nm) is due to interband transition of copper electron from deep level of valence band [18] and CuO nanoparticles [19] an absorption peak at 740 nm which corresponds to the surface plasmone resonance peak of CuO nanoparticles and belonged to a greenish color of the sample [20].

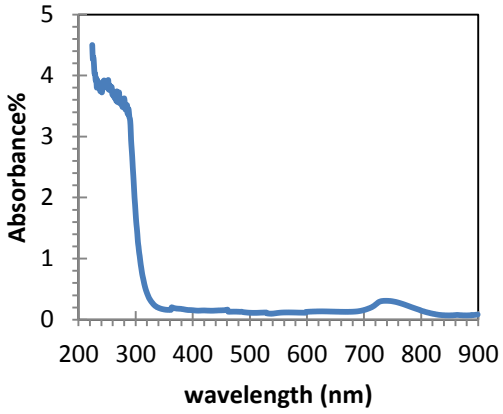

(a)

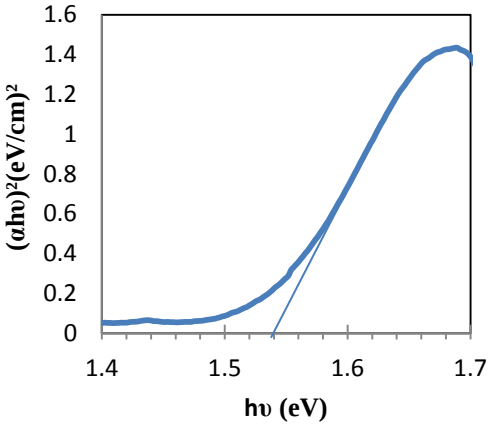

(b)

Fig.(4(a)): Absorption spectrum of CuO nanoparticles, (b) optical band gap of CuO nanoparticles synthesis by laser ablation in DIW.

The value of the optical band gap energy can be account in the direct allowed state transitions, any gap energy is gap between the top of valence band and bottom conduction band when the wave vector K equal to zero by equation, which connected between the absorption coefficient (α) and energy band gap (E_g) [22].

$$(\alpha h\upsilon) = B(h\upsilon - Eg)^{½} \quad \text{..... (1)}$$

By plotting between $(\alpha h\upsilon)^2$ against $h\upsilon$ as shown in the Fig.(4b), the direct band gap (Eg) is determined from the intercept of the straight line touches of the curve in the x-axis at $(\alpha h\upsilon)^2$ equal zero found to be 1.54 eV. This result is larger than the band gap of the CuO bulk. The increase is denoting of quantum confinement effect [23]. The result of the band gap demonstrates that the CuO absorbs at infrared region at most as a narrow band gap semiconductor. In order to make the absorbance in visible region, the dopping with gold nanoparticles must be done.

Fig.(5a,b) indicates the UV-visible absorption spectrum of Au:CuO nanocomposite after soldering and the variation of $(\alpha h\upsilon)^2$ as a function of photon energy ($h\upsilon$) respectively. The absorption peak at 527 nm could be recognize of Au:CuO nanoparticle and the optical direct band gap is about 1.95 eV.

The band gap of pure CuO nanoparticles and Au doped CuO are about 1.54 eV and 1.95 eV respectively, therefore the optical spectrum blue shift corresponding to the increasing of the band gap, the increasing in the band gap can be described as a result to the (Burstein. Moss shift). As the nearby levels of conduction band is full by electrons, so that the electrons need to more energy for moving, it seems as if the energy gap increases [24]. The additional absorption are observed in the visible region of Au doped CuO these results indicate that copper oxide can be activated by visible light and Au doping could become one of the more important factor influencing the photovoltaic activity of CuO nanoparticles [25].

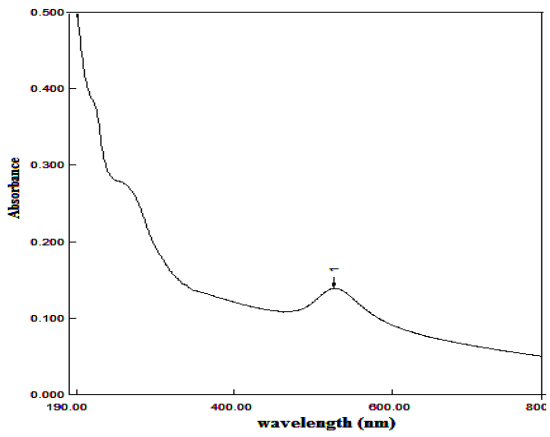

(a)

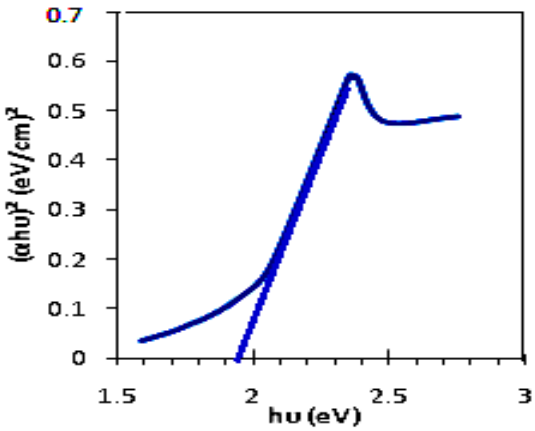

Fig.(5): (a) The absorption spectrum of Au:CuO nanoparticles, (b) band gap of Au:CuO nanoparticles synthesis by laser soldering in DIW.

2-Zeta potential measurement

Zeta potential is important term can be used to indicate the stability of nanoparticles colloidal [26]. The stability of Au:CuO nanocomposite in aqueous solution is very associated to its electro kinetic properties, Well-dispersed colloidal could be obtain with high surface charge density to produce strong repulsive forces. The repulsion between particles becomes strong and the stability of particles increases as the absolute value of zeta potential increases. On the contrary, it become easy to precipitate particles as zeta potential becomes near to zero [27].

Fig.(6 a) indicates the zeta potential of Au: CuO nanocomposite in DIW, it has a maximum peak at -54 mV, it indicates that the negatively charged of Au: CuO nanocomposite in DIW. The amount of zeta potential is nearest to 60 mV indicating that the colloid is good stability against aggregation [28] and well dispersed in DIW as a result to the t presence of the ionic characteristic for micelles, the electrostatic repulsive forces between nanoparticles in water suspension prevent them from agglomeration and sedimentation [29]. Figs. (6 b, c) illustrates the mobility and the frequency shift of Au:CuO nano colloidal respectively.

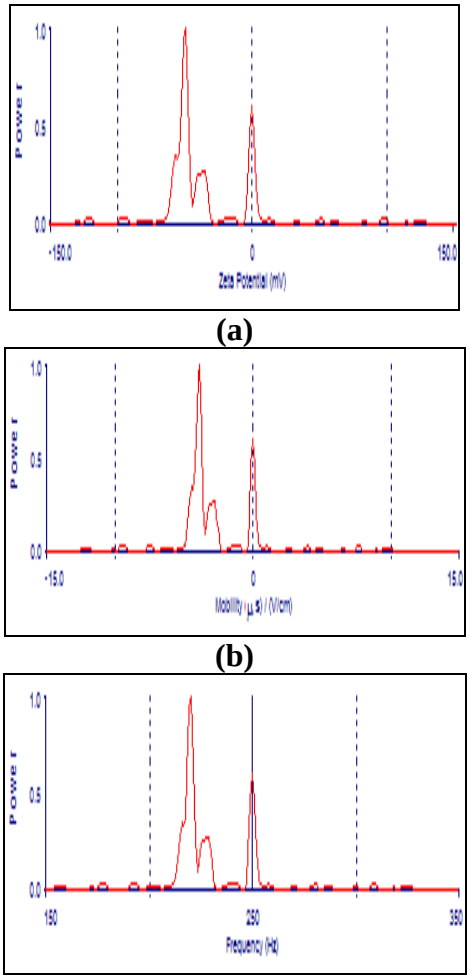

Fig.(6): (a) The zeta potential, (b) the mobility and (c) the frequency shift of Au: CuO nanocolloidal synthesis by laser soldering in DIW.

3-Surface morphology

Atomic force Microscope is ideally used for characterization the surface morphology of Au:CuO nanocomposite prepared by laser soldering, its offer information about physical properties including size and morphology of nanoparticles.

Fig.(7 a) show the 2–dimension and 3-dimension topography image of the Au:CuO nancomposite synthesis by laser soldering in DIW. The bright points in the image show the nanoparticles and the intensity of color reflects the height of the particles.

The amplitude parameters, the root mean square, and ten point height and roughness average were obtained from two dimensional topography are 1.14, 2.48 and 0.97 nm respectively. Three dimension image give a rows and columns of nearly spherical shape and homogeneous particles.

Fig.(7 b) show granularity accumulation distribution of Au:CuO nanocomposite, this figure show a large number of particles have diameter approximately 55 nm.

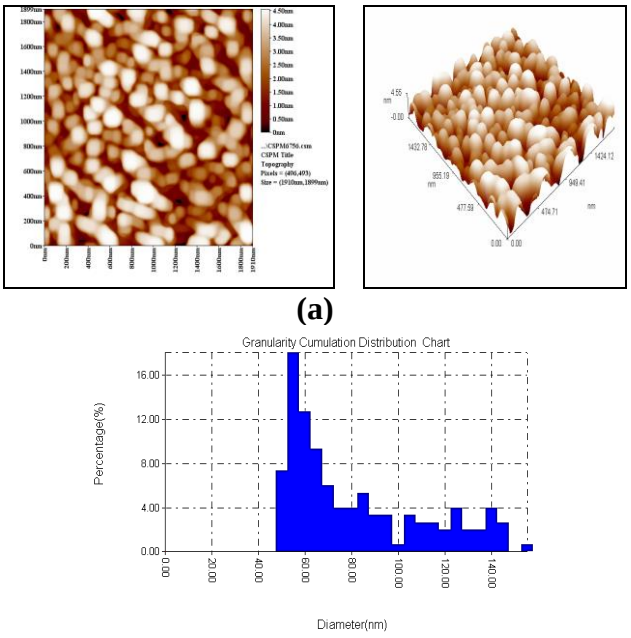

Fig.(7): (a) 2D, 3D AFM image, (b) granularity accumulation distribution of Au:CuO nancomposite synthesis by laser soldering in DIW.

4-X-Ray Diffraction pattern

The X-Ray diffraction pattern of Au:CuO nancomposite synthesis by laser soldering in DIW deposited on porous silicon is indicated in Fig.(8).

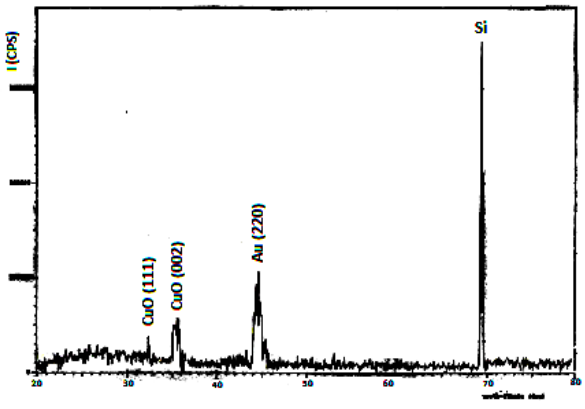

Fig.(8): X-Ray Diffraction pattern of Au:CuO nancomposite synthesis by laser soldering in DIW deposited on porous silicon.

Fig.(8) shows several diffraction peaks can be observed at (2θ) = 32.5° and 35.6° corresponds to (111) and (002) lattice planes

of data monoclinic phase of CuO confirmed by standard JCPDS data (card No. 02-1225) [30]; Peak at 44.48° angle is clearly observed assigning to (2 2 0) lattice planes of face-centered cubic (FCC) structure of metallic gold according to standard data (JCPDS No. 04-0784) [31], the Broadening of XRD peaks clearly indicate that the Au NPs and CuO Nps are nanocrystalline in nature.

II-Characterization of porous silicon

Fig.(9 a) indicates the atomic force microscope image of the porous silicon, the surface of the PS layer was a sponge-like structure which consists of a lot of numbers of 'pores' and 'voids'. These 'pores' and 'voids' make porous silicon an adhesive surface for accommodating of Au: CuO nanoparticles into its pores. In Fig.(9 a), the features of the pores are clear. The most common, the shape of pore is spherical and oval; the average pore diameter is 77 nm so that the PS layer is macro porous silicon.

Fig.(9 b) is the granularity accumulation distribution of porous silicon. AFM measurement can give information about the porous silicon layer as shown in Table (1).

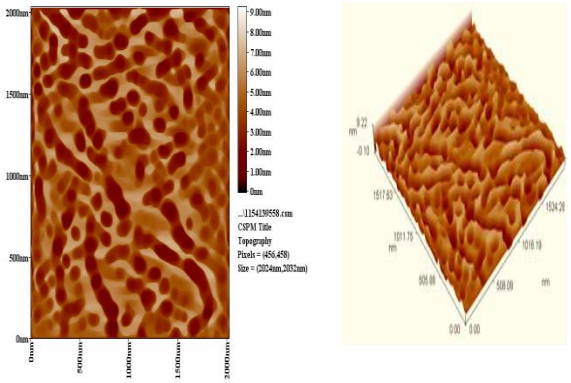

(a)

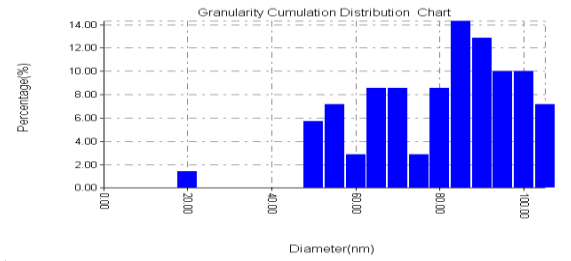

(b)

Fig.(9):(a) 2D, 3D AFM image, (b) granularity accumulation distribution of porous silicon prepared at 532nm wavelength green laser with power 30 mW, etching time 3 min and current 10 mA at 25% HF concentration.

Table (1)
Information about the porous silicon layer from AFM measurement.

parameter	(nm)
roughness average	1.2
root mean square	1.43
ten point height	3.26
surface area ratio	0.575
number of pores	70
average pore diameter	77
depth	4.23

III-Characteristic of Au:CuO/ porous silicon hetrojunction

1-Current –Voltage characteristic in the dark

Current – voltage (I-V) characteristic of p-n junction give important information to judge the performance, rectification behavior and ideality factor of the fabricated diode.

Fig.(10) represents the current–voltage characteristic of Au:CuO nanocomposite on porous silicon hetrojunction at forward and reverse base in dark at room temperature.

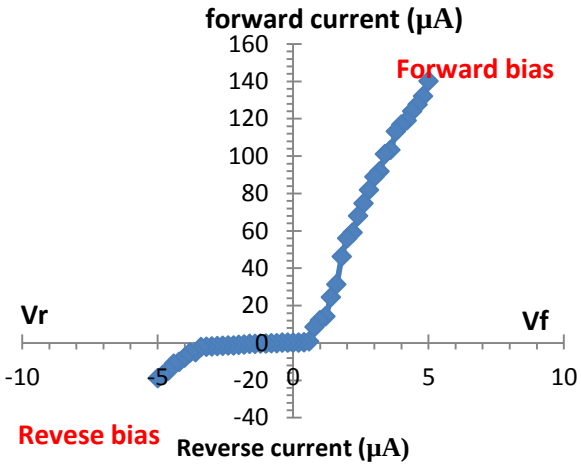

Fig.(10): Current-voltage in forward and reverse bias of Au:CuO nanocomposite/ porous silicon hetrojunction in the dark at room temperature.

When shine a positive voltage across the depletion region, lead to minimize the internal electric field across the depletion region down by bias voltage, due to increase the diffusion current compared with the drift current. When the applied voltage is less than the potential barrier, the forward current is very slightly

increase with the applied voltage until become 0.8 volt, the forward current increases exponentially as a result that the applied voltage in forward bias exceeds the internal barrier potential, this bias voltage gives energy to the electrons make them to overcome on the barrier height and flow the current called diffusion current.

In opposite bias, it is clear that no increase in the current with increase of the applied voltage but when the voltage reach to 3.6 volt, the current is a significant increase with applied voltage, This current is produced from the diffusion of minority charge carriers through the depletion region, this tend to generate on electron-hole pairs.

The rectification ratio (RR) of fabricated diode can be determined at a certain applied voltage on the diode as the ratio between the passage current when diode connect in the forward bias to the passage current in reverse bias (IF/IR) **[32]**. The rectification ratio (RR) of Au:CuO nanocomposite/ porous silicon is 46.66 at ±2 V and a low turn-on voltage of 0.8 V can be achieved for the device in dark, such RR was ascribed to the electron mobility of Au:CuO NC.

Diode resistance would be defined as function of the dark current and the applied bias, its the variation as a function of applied bias and its given from equation [33].

$$R_d = \left(\frac{dV}{dI}\right) \quad \text{..... (2)}$$

Diode resistance is shown in Fig.(11).

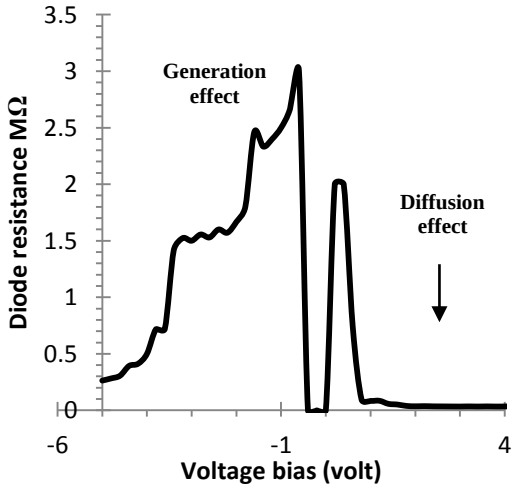

Fig.(11): The variation of diode resistance via voltage bias in the dark current.

The value of the ideality factor of the heterojunction can be determined by plotting between forward bias voltage and log of forward current as shown in the Fig.(12), the value of the ideality factor of this hetrojunction can calculated by using the equation [34].

$$n = \frac{q}{kT} \cdot \frac{\partial V}{\partial \ln I} \quad \text{..... (3)}$$

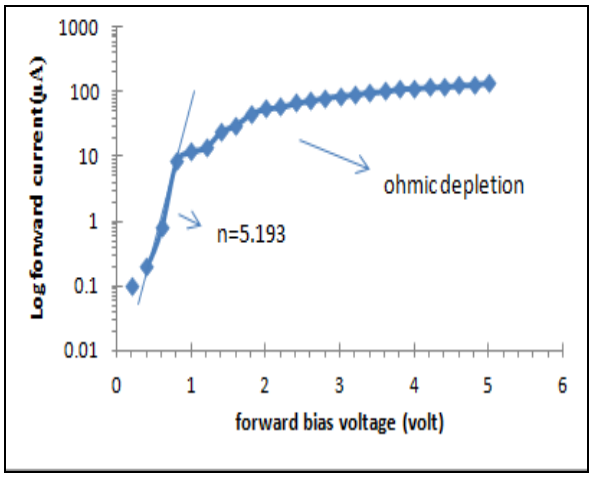

Fig.(12): Semi-log current–voltage characteristic in forward bias.

The turn-on voltage for the Au:CuO nanocomposite/ porous silicon hetrojunction is about 0.8 V, The ideality factor and reverse saturation current are 5.193 and 20×10^{-6} A respectively. The value of ideality factor is larger than unity which can be associated to recombinatted of electrons and holes in the depletion region as well as the mismatch beween Au:CuO NC and porous silicon is very high and then increase the density of trap state.

2- Current-Voltage under illumination

Au:CuO/ porous silicon hetrojunction is work as photodiode in reverse bias and under illumination by white light lamp at different power per unit area as shown in Fig.(13).

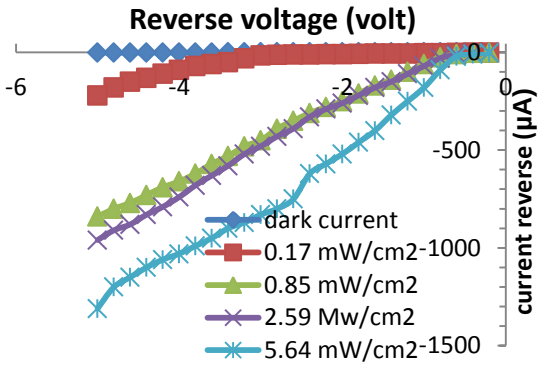

Fig.(13): Current-voltage in reverse bias of Au:CuO/ porous silicon hetrojunction under illumination with different intensity of the light.

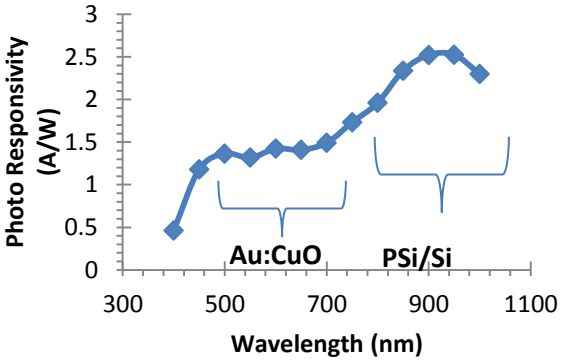

Fig.(14): Responsivityas function of wavelength for Au:CuO/ porous silicon hetrojunction at reverse bias voltage of – 2.5 Volt.

The photocurrent is larger than the dark current in reverse bias, This increase is mainly as a result of the expansion in the depletion region, therefore more incident photons will contribute to the generation of the electron-hole pairs in the depletion region, the depletion region able to separate the electron- hole pair generated from each other by internal electric field more efficiency. Where the large incident intensity refers to the number of incident photons are large and its lead to increase the superstation of electron-hole pairs and the increase of the photocurrent. This phenomenon allows the diode to be used as a switch or relay when sufficient light is present.

3- Photoresponsivity

The photocurrent generated depend on the incident wavelength on the photodetector in reverse bias**,** responsivity can be determined by as the proportion between the current passing through the detector in reverse bias and the incident light power at a given wavelength on the photodector. The responsivity R_λ of Au:CuO/ porous silicon hetrojunction as function of wavelength at 2.5 volt reverse bias and can calculated by equation [35].

$$R_\lambda = \frac{I_{Ph}}{p_{in}} \quad \text{..... (4)}$$

Where I_{ph}: is the current passing through the photodetector under illumination using a halogen lamp, and monochromatic to obtain on the electromagnetic spectrum from 375nm-1000nm, P_{in} is the light power of incident wavelength.

Fig.(14) represents the curve of the photoresponsivity as function of incident wavelength on the Au:CuO/ porous silicon hetrojunction, it is noticeable that the response curve contain two regions , the first one is located between (450nm-650nm) wavelength corresponding to the near violet-visible spectral region. This decline in the responsivity curve due to the absorption light in porous layer (toward PS/n-Si side of Au:CuO /PS/n-Si/Al heterojunction). Second region represents the peak located at the wavelength 750-1100 nm related to band edge absorption in silicon substrate [37]. These regions formed as a result the indirect band gap of silicon approximately 1.1 eV is smaller than of dirct band gap of porous silicon is (2 to 3 eV). Thus the wavelength cut –off of p Si is smaller than wavelength cut –off of silicon substrate, for this the porous layer of silicon absorbed the light have shorter wavelength (UV-Visible) comparable with bulk silicon which absorbed the light have larger wavelength (near infrared) [37].

4-Quantum efficiency

Quantum efficiency can be defined as the number of electron – hole pairs generated for each incident photon, and can be given by the following formula [35].

$$Q.E = 1240 \frac{R_\lambda}{\lambda} \quad \text{..... (5)}$$

Where R_λ is the responsivity of the hetrojunction, which is result of current generation from absorption of incident light wavelength. Quantum efficiency depends

mainly on the value of absorption coefficient, which in turn depends on the wavelength of the incident on the hetrojunction.

It is noted that the value of quantum efficiency region (violet-visible) is higher than 100%, the silicon pores represented as non reflect layer, this result is due to the absorption of light is higher in the porous layer, and the transmission at the roughness of porous and bulk interfaces leads to reduce of light reflection. This parameter has its significant role in order to enhance the light. High value of quantum efficiency (large than 100%) come from the surface of porous silicon is very roughness; High value of quantum efficiency (large than 100%) come from several reasons, (1) abundant reactive sites on the surface induced by quantum confinement effect, (2) internal gain of the photoconductor and (3) multiple electron injection and collection per incident photon [38]. Finally may be from avalanche effect inside the porous silicon and the voltage drop in porous silicon which is intrinsic and as narrow as silicon [39].

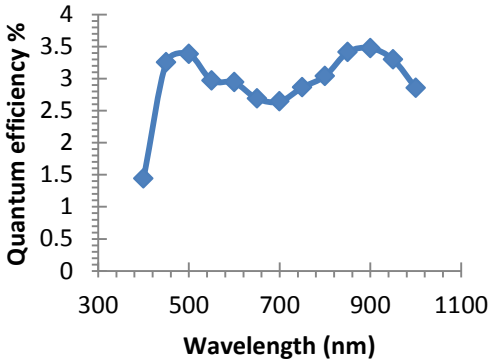

Fig.(15): Quantum efficiency as function of wavelength for Au:CuO/ porous silicon hetrojunction at reverse bias voltage of – 2.5 Volt.

Conclusions

The purpose of the present work is to synthesize of Au:CuO NC and to study the optical, stability, structural and surface morphology characteristics. The band gap of pure CuO nanoparticles and Au doped CuO are about 1.54 eV and 1.95 eV respectively, therefore the optical spectrum blue shift corresponding to the increasing of the band gap, zeta potential is indicating that the negatively charged of Au: CuO nanocomposite in DIW. The amount of zeta potential is 54 mV indicating that the colloid is good stability against aggregation. surface morphology includes the root mean square, ten point height and roughness average were 1.14, 2.48 and 0.97 nm respectively. Granularity accumulation distribution of Au:CuO nanocomposite show a large number of particles have size about 55 nm. While the average pore diameter of porous silicon is 77 nm so that the PS layer is macro porous silicon.

Au: CuO nanocomposite deposited on porous silicon by drop casting technique for preparation of silicon photodetector, the electrical properties prove that band gap alignment between Au: CuO nanocomposite and PS facilitates the electron transfer and further increases the photoresponsitivity and Quantum efficiency.

Reference

[1] Ali Shrifian-Esfahni, Mohammad Taghi Salehi, Mojtaba Nasr-Esfahni and Ehsan EKRAMIAN, "Chitosan-modified superparamgnetic iron oxide nanoparticles: design, fabrication, characterization and antibacterial activity", Science, 69(1), 26–32, 2015.

[2] Li, Y., Song, Y.Y., Yang, C. & Xia, X. H. "Hydrogen bubble dynamic template synthesis of porous gold for nonenzymatic electrochemical detection of glucose" Electrochem. Commun., 9, 981-988, 2007.

[3] Jalal A., Amir A., "Novel metal oxide nanocomposite Au/CuO-ZnO for recyclable catalytic aerobic oxidation for alcohols in water", catalysis communication, 49, 1-5, 2014.

[4] Lanlan S., Dongxu Z., "A white-emitting ZnO-Au nanocomposite and SERS application", applied surface science, 258(20), 7813-7819, 2012.

[5] Davide Barreca, Giorgio Carraro, "Novel Synthesis and Gas Sensing Performances of CuO–TiO_2 Nanocomposites Functionalized with Au Nanoparticles" J. physical chemistry C, 115(21), 10510-10517, 2011.

[6] S.N.Grigoriev, V.Yu Fominski, "Puled laser deposition of nano composite MoSex/Mo thin film catalysts for hydrogen evolution reaction", Science Direct journal, part A, 592, 175-181, 2015.

[7] Geetika Bajaj, R. K. Soni, "Synthesis of composite gold/tin-oxide nanoparticles by nano-soldering" J Nanopart Res, springer, DOI 10.1007/s11051-009-9836-2, 2010.

[8] Giuseppe C., Elena M., "Laser synthesis of Au/Ag colloidal nano-alloys: Optical properties, structure and composition", Science Direct journal Applied Surface Science, 254, 1007–1011, 2007.

[9] Jin Z., Michael P., "Laser-Assisted Synthesis of Superparamagnetic Fe@Au Core-Shell Nanoparticles", J. Phys. Chem. B, 110, 7122-7128, 2006.

[10] Yoshie Ishikawa, Kenji Kawaguchi, "Preparation of Fe–Pt alloy particles by pulsed laser ablation in liquid medium, Chemical Physics Letters", 428, 426–429, 2006.

[11] Zhu, H., Lu, X., Li, M., Shao, Y. & Zhu, Z. "nonenzymatic glucose voltammetric sensor based on gold nanoparticles/carbon nanotubes/ionic liquid nanocomposite", Talanta, 79, 1446-1453, 2009.

[12] Nittaya T., Chaikarn L., "Synthesis of Thermally Spherical CuO Nanoparticles" Hindawi Publishing Corporation, Journal of Nanomaterials, 2014, Article ID 507978, 1-5, 2014.

[13] Jiahuan Lei, Yu Liu, Au/CuO "nanosheets composite for glucose sensor and CO oxidation", RSC Advances, An international journal to further the chemical sciences, 5(12), 9130-9137, 2015.

[14] Jaya Pal, Mainak G., "Hierarchical Au–CuO nanocomposite from redox transformation reaction for surface enhanced Raman scattering and clock reaction", Cryst. Eng.Comm. (Impact Factor: 4.03); 16(5), 883–893, 2013.

[15] R. S. Dubey, "Electrochemical Fabrication of Porous Silicon Structures for Solar Cells" Nanoscience and Nanoengineering, 1(1), 36-40, 2013.

[16] C.F. Boren, D.R. Huffman, "Absorption and Scattering of Light by Small Particles", Wiley, New York, 1983.

[17] Dongfang Y., Seongkuk L., Bo CHEN and Suwas N., "Fabrication of Gold Nanoparticles by Pulsed Laser Ablation in Aqueous Media", JLMN-Journal of Laser Micro/Nanoengineering, 3(3), 147-151, 2008.

[18] R K Swarnkar, S C Singh and R Gopal, "Effect of aging on copper nanoparticles synthesized by pulsed laser Ablation in water: structural and optical characterizations", Bull. Mater. Sci., 34(7), 1363–1369, 2011.

[19] Ho Chang1, Xin-Quan Chen, Ching-Song Jwo, and Sih-Li Chen, "Electrostatic and Sterical Stabilization of CuO Nanofluid Prepared By Vacuum Arc Spray Nanofluid Synthesis System (ASNSS)", Materials Transactions, 50(8), 2098 - 2103, 2009.

[20] Tran X. Phuoc, Minking K. Chyu, Synthesis and Characterization of Nanocomposites Using the Nanoscale Laser Soldering in Liquid Technique Journal of Materials Science & Nanotechnology, Journal of Materials Science & Nanotechnology, 1(1), 1-5, 2013.

[21] N.F. Mott, E.A. Davies, "Electronic Processes in Non-Crystalline Materials", Clarendon Press, Oxford, 1979.

[22] P. Mallick, S. Sahu, "structure, microstructure and optical absorption analysis of CuO nanoparticles synthesized by sol-gel route", nanoscience and nanotechnology journal, 2(3), 71-74, 2012.

[23] S. G. Rejith and C. Krishnan, "Synthesis of cadmium-doped copper oxide nanoparticles: Optical and structural characterizations" Advances in Applied Science Research, 4(2), 103-109, 2013.

[24] R. Ferro and J. A. Rodriguez, "Study of Some Optical Properties of CdO:F Thin Films", J. Physica Status Solidi (b), 220, 299-304, 2000.

[25] Qingwei z., yihe Z., Jiajun W., "Microwave Synthesis of Cuprous Oxide Micro-/Nanocrystals with Different Morphologies and Photocatalytic Activities", Journal Material Science Technology, 27, 289-295, 2011.

[26] Soheyla H., Foruhe Z., "Effect of Zeta Potential on the Properties of Nano-Drug Delivery Systems - A Review (Part 2)", Tropical Journal of Pharmaceutical Research, 12(2), 265-273, 2013.

[27] M. Sahooli, S. Sabbaghi, M. Shariaty Niassar, "Preparation of CuO/Water Nanofluids Using Polyvinylpyrolidone and a Survey on Its Stability and Thermal

Conductivity", Int. J. Nanosci. Nanotechnol., 8(1), 27-34, 2012.

[28] Green w., R; Kendall, "Electroacoustic studies of moderately concentrated colloidal suspensions". Journal of the European Ceramic Society, 19(4), 479–488, 1999.

[29] Der-Chi Tien, Liang-Chia Chen, Nguyen Van Thai, and Sana Ashraf, "Study of Ag and Au Nanoparticles Synthesized by Arc Discharge in Deionized Water", Hindawi Publishing Corporation Journal of Nanomaterial, 2010, 1-9, 2010.

[30] N. Bouazizi1, R. Bargougui, A. Oueslati, R. Benslama, "Effect of synthesis time on structural, optical and electrical properties of CuO nanoparticles synthesized by reflux condensation method", advanced materials letters, 6(2), 158-164, 2015.

[31] Pradnya N., Tulsi M., Sudhir K., "Green Synthesis of Gold Nanoparticles Using Glycerol as a Reducing Agent", Advances in Nanoparticles, 2(2), 10894- 10900, 2013.

[32] Z. AHMAD, M. H. SAYYAD, "Electrical characteristics of a high rectification ratio organic Schottky diode based on methyl red", optoelectronics and advanced materials–rapid communications, 3(5), 509 – 512, 2009.

[33] M. Özer, D.E. Yıldız, Ş. Altındal, "Temperature dependence of characteristic parameters of the Au/SnO_2/*n*-Si (MIS) Schottky diodes", Solid-State Electronics, 51(6), 941–949, 2007.

[34] Salah E. El-Zohary, M. A. Shenashen, 1 Nageh K. Allam, T. Okamoto, and M. Haraguchi, "Electrical Characterization of Nanopolyaniline/ Porous Silicon Heterojunction at High Temperatures", Hindawi Publishing Corporation Journal of Nanomaterials, 2013, Article ID 568175, 1-8, 2013.

[35] Raid a. Ismail, "characteristics of p-cu2o/n-si heterojunction Photodiode made by rapid thermal oxidation", journal of semiconductor technology and science, 9(1), 51-54, 2009.

[36] Chia-Man Chou, Hsing-Tzu Cho, Vincent K S Hsiao, Ken-Tye, "Quantum dot-doped porous silicon metal–semiconductor metal photodetector" Nanoscale Research Letters, 7(291),1-4, 2012.

[37] S. V. Svechnikov, E. B. Kaganovich, E. G. Manoilov, "Photosensitive porous silicon based structures" Semiconductor Physics, Quantum Electronics & Optoelectronics,1 (1),13-17. 1998.

[38]- Fawen Guo, "Low Noise, High Detectivity Photodetectors based on Organic Materials", Ph.D. University of Nebraska, 2014

[39] Hasan A. Hadi, Faten Sh. Zain Al-Abedeen, "Comparative Study in Optoelectronic Properties between Nano Gold/Porous Silicon Heterojunction Based on P and N-Type Crystalline Silicon", International Journal of Emerging Research in Management &Technology, 3(11), 166-171, 2014.